Few-Body Syst (2018) 59:110
https://doi.org/10.1007/s00601-018-1430-7

T. Cao · Y. Ilieva · N. Zachariou on behalf of the CLAS Collaboration

Determination of the Polarization Observables C_x, C_z, and P_y for the Quasi-Free Mechanism in the Reaction $\vec{\gamma}\, d \to K^+ \vec{\Lambda}\, n$

Received: 8 April 2018 / Accepted: 20 June 2018

Abstract The study of the excited-nucleon (N^*) spectrum is fundamental for the quest to understand non-perturbative quantum chromodynamics. Measured kinematical evolutions of experimental observables, such as polarizations and unpolarized cross sections, for exclusive meson photoproduction off proton and neutron, are the foundation of theoretical and phenomenological analyses that identify the N^* states excited in these reactions and determine their parameters. While free proton targets are readily available, experiments typically use bound neutrons, such as in the deuteron, to estimate observables for photoproduction off the free neutron. Even though exclusivity allows to select event samples dominated by quasi-free scattering (QF), it is not clear if the obtained observables are unbiased estimates of the observables for photoproduction off the free neutron. Studies assessing the possible sources of bias, such as the neutron binding and final-state interactions (FSI), are sparse and primarily focused on the unpolarized cross sections. The comparison between observables for production off the free and off the bound proton in high-statistics reactions, seems to be the natural way to study and to quantify these effects experimentally. Alternatively, one can map the evolution of the QF observables with target-neutron momentum and potentially extrapolate it to the "free"-neutron point of zero momentum. In this work, we determine the recoil polarization P_y of the Λ hyperon and the polarization transfers C_x and C_z from circularly-polarized photons to the Λ for the quasi-free mechanism of the reaction $\vec{\gamma}\, d \to K^+ \vec{\Lambda}\, n$, i.e., for photoproduction off the bound proton. The data were taken with the CLAS detector at the Thomas Jefferson National accelerator facility (JLab) during the E06-103 (g13a) experiment and cover E_γ between 0.9 and 2.6 GeV and $\cos\theta_{KCM}$ between -0.3 and 0.8. For several kinematic bins, the dependence of the polarizations on the target-proton momentum is studied. Our work can be used as a benchmark to develop analysis strategies to reduce potential bias due to FSI and the binding of the neutron in the deuteron in reported polarization observables for quasi-free meson photoproduction off the bound neutron.

This work is funded in part by the U.S. NSF under Grant PHY-1505615.

This article belongs to the Topical Collection "NSTAR 2017 – The International Workshop on the Physics of Excited Nucleons".

T. Cao (✉)
Hampton University, Hampton, VA, USA
E-mail: caot@jlab.org

Y. Ilieva
University of South Carolina, Columbia, SC, USA
E-mail: jordanka@physics.sc.edu

N. Zachariou
University of Edinburgh, Edinburgh, UK
E-mail: nick.zachariou@ed.ac.edu

Published online: 10 July 2018

1 Introduction

Exclusive meson photoproduction off the neutron is of significant value in the study of nucleon resonances and the search of missing resonances as some excited states are predicted to couple strongly to the neutron. Since free neutron targets do not exist, and due to the weak binding of the deuteron, the latter is often used as a neutron target. In order to study the effects of nucleon binding and final-state interactions, we extract polarization observables for $K^+\Lambda$ photoproduction off the bound proton and demonstrate an experimental method to quantify the bias of an observable extracted from such data compared to the observable for production off the free proton. We consider $K^+\Lambda$ production off the proton since the number of $K^+\Lambda$ events in the E03-106 data set is much higher than the number of $K^0\Lambda$ events from photoproduction off the bound neutron. The higher statistics allows us to map the dependence of the observables on the target-proton momentum for different kinematic bins.

The reaction we consider is, thus, $\vec{\gamma}\, d \rightarrow K^+ \vec{\Lambda} n$. In a simple picture, this reaction can be understood in terms of single- and double-step two-body-to-two-body processes (see Fig. 1).

The QF scattering (top left diagram) is the mechanism that is of interest for the N^* program. In this single-step mechanism, the incoming photon couples to the bound proton to produce the final-state K^+ and Λ particles. The neutron in the deuteron acts as a spectator (does not participate in the reaction) and scatters off carrying its Fermi momentum. The other three diagrams in the figure show two-step mechanisms involving both nucleons in the deuteron. In these final-state interactions, the incident photon interacts in the first step with one of the target nucleons, which produces a meson and a baryon. In the second step one of these two particles scatters off the other target nucleon. While the QF mechanism dominates the cross section of the reaction of interest, FSI can have a significant contribution at some kinematics, such as high spectator momenta. Besides, FSI dilute the polarization observables for the QF mechanism and can lead to a systematic bias if these observables are used as estimates of the observables for production off the free nucleon.

We make use of the exclusivity of the measurement to obtain an event sample dominated by QF events and an event sample dominated by FSI events. This is achieved by making use of the fact that in QF production the final-state neutron momentum, p_n, is predominantly low and consistent with the typical nucleon Fermi momentum in the deuteron, while final-state neutrons that have taken part in a final-state interaction carry larger momenta. For the purpose of this study, we classify all $K^+\Lambda n$ events with $p_n < 200$ MeV/c as QF events and we extract the polarization observables C_x, C_z, and P_y from this QF sample. The events with $p_n > 200$ MeV/c are classified as FSI events. The observables extracted from the FSI-dominated sample provide complementary information at high neutron momenta.

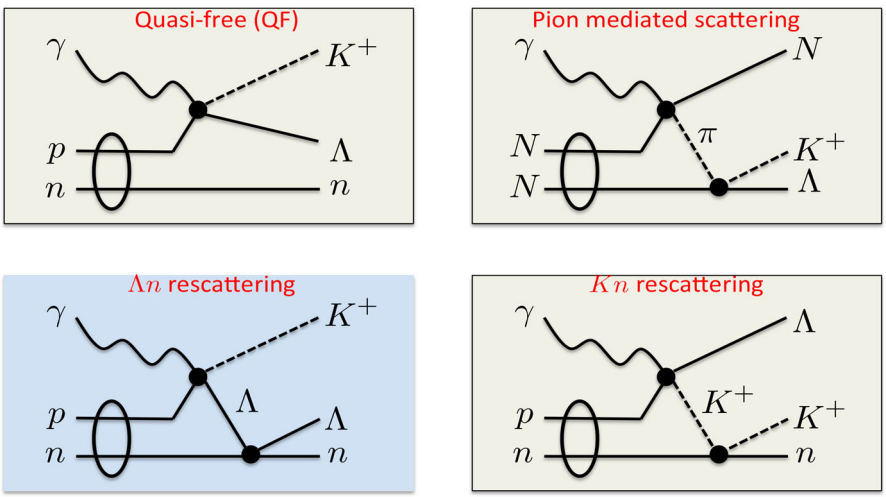

Fig. 1 The four main mechanisms contributing to the reaction $\vec{\gamma}\, d \rightarrow K^+ \vec{\Lambda} n$. The diagrams showing quasi-free scattering (top left), pion-mediated production (top right), Λn rescattering (bottom left) and Kn rescattering (bottom right) all describe final-state interactions

2 Experiment and Data Reduction

The data for this study were collected with the CLAS [1] at JLab during the g13 experiment [2]. A circularly-polarized tagged real-photon beam, with polarization of 30–80% and energy between 0.5 and 2.5 GeV, was generated in the Hall-B tagging facility [3]. The photons were incident on a 40-cm-long unpolarized liquid deuterium target located 20-cm upstream of the center of the CLAS. While the final-state K^+ was directly detected, the Λ hyperon was identified by detecting the $p\pi^-$ pair from the $\Lambda \rightarrow p\pi^-$ decay and forming the invariant mass of the pair, $M_{p\pi^-}$. The event distribution over $M_{p\pi^-}$ shows a narrow peak around the nominal mass of the Λ. Events yielding an invariant mass outside of the Λ peak were excluded from further analysis.

In order to select the exclusive $K^+\Lambda n$ events, the 4-vector of the missing state in the reaction $\gamma d \rightarrow K^+\Lambda X$ was reconstructed by means of four-momentum vector conservation

$$\tilde{p}_X = \tilde{p}_\gamma + \tilde{p}_d - \tilde{p}_{K^+} - \tilde{p}_\Lambda, \tag{1}$$

where $\tilde{p}_\gamma$, $\tilde{p}_d$, $\tilde{p}_{K^+}$, and $\tilde{p}_\Lambda$ denote the four-momentum vectors of the incident photon, the deuteron, the final-state kaon, and the final-state hyperon, respectively. The event distribution over the invariant mass of the missing state, $M_X = \sqrt{|\tilde{p}_X|^2}$, exhibits a peak around the nominal neutron mass. The final $K^+\Lambda n$ data sample consists of the events in the peak after estimating and removing the amount of background events under the peak. The final data sample is then divided into a quasi-free-dominated sample and a final-state-interaction-dominated sample by applying a cut on the value of p_X, as described earlier. The observables C_x, C_z, and P_y for the quasi-free scattering and for the FSI mechanisms are then obtained simultaneously from a maximum log-likelihood fit to these final samples. More details about the definition of axes, selection of events, and extraction of observables can be found in [4].

3 Results and Discussion

Our results for the observables C_x, C_z, and P_y for the quasi-free photoproduction of $K^+\Lambda$ off the proton bound in a deuteron are shown in Figs. 2, 3, and 4, respectively. The data are reported for kinematic bins in photon energy, E_γ, and cosine of the kaon polar angle in the $K^+\Lambda$ center-of-mass system, $\cos\theta_{KCM}$.

One of the main sources of bias for the QF observables (when compared to results for scattering off the free nucleon) is the contribution of FSI events with neutron momenta below 200 MeV/c that are not removed by the neutron-momentum cut. We quantified the amount of FSI events in our QF sample by means

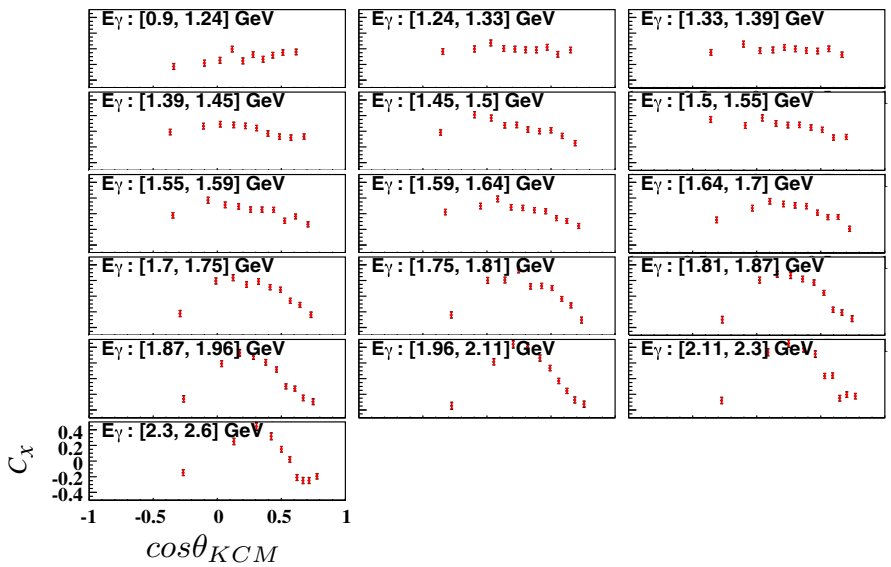

Fig. 2 C_x as a function of $\cos\theta_{KCM}$ at fixed E_γ. The $\cos\theta_{KCM}$ values at which our results for C_x are reported, are the averages of the $\cos\theta_{KCM}$ values of all the events in the corresponding E_γ and $\cos\theta_{KCM}$ bins. The inner red error bars denote statistical uncertainties and the outer black error bars denote total uncertainties

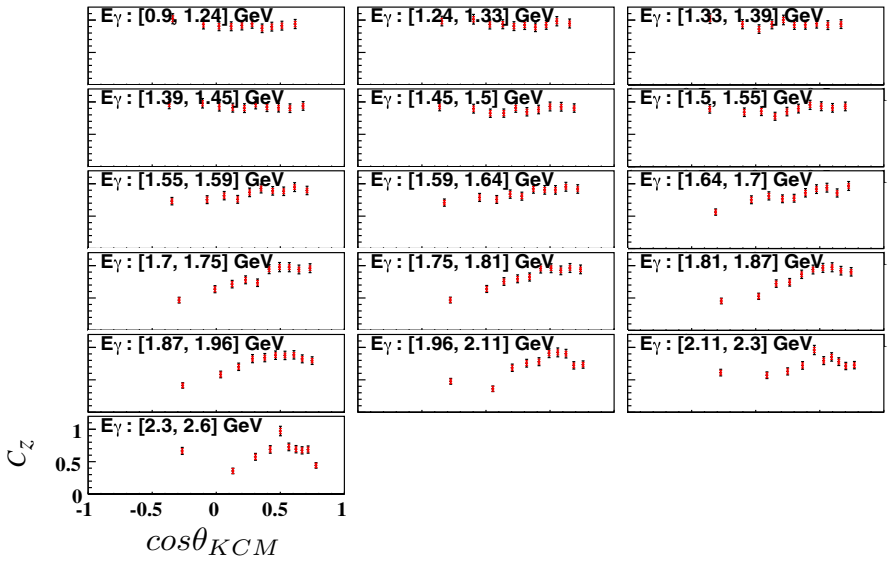

Fig. 3 C_z as a function of $\cos\theta_{KCM}$ at fixed E_γ. The $\cos\theta_{KCM}$ values at which our results for C_z are reported, are the averages of the $\cos\theta_{KCM}$ values of all the events in the corresponding E_γ and $\cos\theta_{KCM}$ bins. The inner red error bars denote statistical uncertainties and the outer black error bars denote total uncertainties

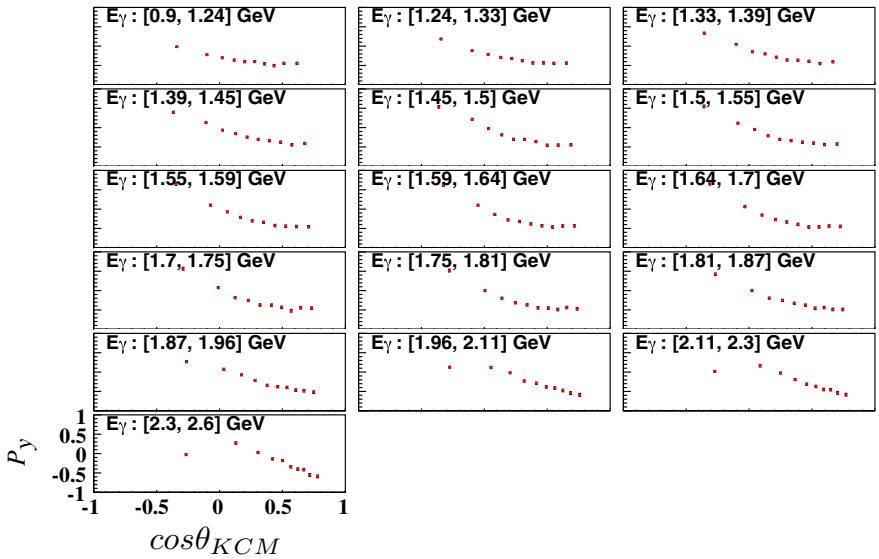

Fig. 4 P_y as a function of $\cos\theta_{KCM}$ at fixed E_γ.The $\cos\theta_{KCM}$ values at which our results for P_y are reported, are the averages of the $\cos\theta_{KCM}$ values of all the events in the corresponding E_γ and $\cos\theta_{KCM}$ bins. The inner red error bars denote statistical uncertainties and the outer black error bars denote total uncertainties

of simulated data. The cross sections for all elementary two-body-to-two-body processes shown on Fig. 1 were implemented in an event generator. In the generator, the *pn* interaction in the deuteron was modelled with the Paris potential [5]. The spectator neutron was considered to be on its mass shell and the target-proton invariant mass was determined from the constraint that the sum of the two nucleon four-momentum vectors equals the deuteron four-momentum vector. The generated events were processed through the CLAS detector simulation [6] and analyzed following the same procedure as applied to the real data [4]. We can then use the final data sample of simulated events to compare with and to study properties of the real data sample. Figure 5 shows the distributions of real events as well as simulated QF and FSI events over p_n. The sum of the QF and the FSI distributions was fitted to the real-data distribution to determine the overall scaling constants for the simulated data.

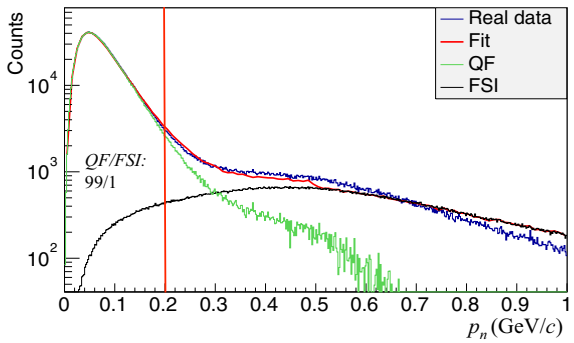

Fig. 5 Neutron momentum distribution for real data (blue), simulated QF production (green), and simulated FSI production (black). The sum of the simulated distributions were fit to the data (red) to determine their overall normalizations. One sees that the contribution of FSI events to the QF sample is about 1% overall. Moreover, the amount of FSI events decreases as p_n decreases

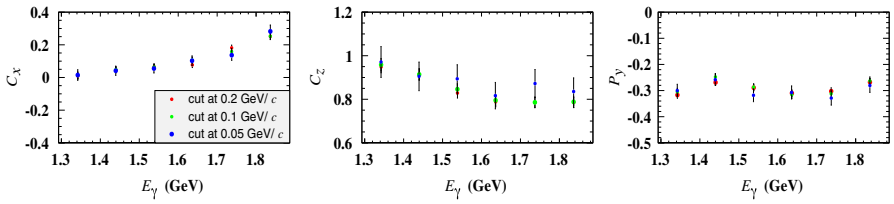

Fig. 6 Observables as a function of E_γ for the $\cos\theta_{KCM}$ bin [0.15, 0.35] for various neutron momentum cuts. The left plot is for C_x, the middle plot is for C_z, and the right plot is for P_y. Red points are for 200 MeV/c cut, green points are for 100 MeV/c cut, and blue points are for 50 MeV/c cut. One should note that the cuts are not exclusive and the statistical uncertainties of the results for the different cuts are not independent

The shape of the simulated distribution matches very well the shape of the data, except for a small discrepancy at neutron momenta above 700 MeV/c. The agreement below 200 MeV/c, which is the range of interest, is excellent. This comparison suggests that we have a reasonable model of the major amplitudes contributing to the reaction unpolarized cross section. While, the relative contribution of FSI would be different for different kinematic bins, their overall contribution to the quasi-free unpolarized cross section is negligible. Although, our estimate of 1% cannot be applied to other quasi-free reactions, it is interesting to note that a theoretical study of the FSI effect on the unpolarized cross section for $\gamma(n) \rightarrow \pi^- p$ extracted from E06-103 data by means of a cut on the spectator proton momentum, finds out that the FSI effect is no larger than 5%, except for the very forward pion scattering angles where the effect can reach up to 30% [7].

To study the effect of FSI specifically on the polarization observables, we do vary the neutron momentum cut. We determine C_x, C_z, and P_y for three different cuts: 200, 100, and 50 MeV/c. Since FSI are expected to dilute the extracted observables and since the amount of FSI events in the QF sample decreases as p_n decreases, we do expect to observe some increase of the magnitude of the polarizations as we narrow the cut. Figure 6 shows a comparison between the estimates of the three observables obtained with different p_n cuts. The comparison is performed for several kinematic bins. The figure suggests that the estimates generally match and that the effect on C_z and P_y may be larger than on C_x. This comparison shows that the selection of QF events by means of a p_n cut of 200 MeV/c is reasonable for the $K^+\Lambda$ reaction.

Since the cut on neutron momentum controls not only the amount of FSI events in the QF sample, but also the target-proton virtuality, we performed a more in-depth study of the evolution of the observables with p_n. In this study, we divided the p_n range into subintervals and determined the observables for each subinterval. Figure 7 shows the evolution of each observable with target-proton momentum (p_p, where $|p_p| = |p_n|$) for different E_γ bins.

Larger p_p correspond to larger proton virtualities, whereas $p_p = 0$ GeV/c corresponds to a free proton. The results are very interesting. Overall, the magnitudes of all QF observables are larger than the magnitudes of the FSI observables. This effect is especially clear when comparing the values at $p_p < 200$ MeV/c with the values at $p_p > 200$ MeV/c. This observation is consistent with the expectation that FSI interactions dilute the polarizations by changing the kinematics of the final-state particles. One also observes that the dependence of C_x, C_z, and P_y on p_p within the QF range of $p_p < 200$ MeV/c is not necessarily a straight line. The shape of the dependence of a given observable varies with E_γ. Also, for the same E_γ, the shape of the dependence

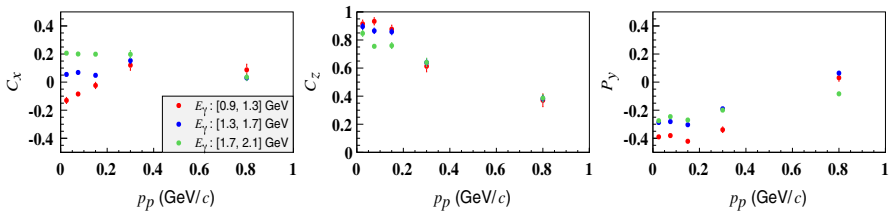

Fig. 7 Observables as a function of target-proton momentum for $0. \leq \cos\theta_{KCM} \leq 0.5$ and different E_γ. Red points show data for the $0.9 \leq E_\gamma \leq 1.3$ GeV, green points show data for the $1.3 \leq E_\gamma \leq 1.7$ GeV, and blue points show data for the $1.7 \leq E_\gamma \leq 2.1$ GeV

is different for the different observables. Since the QF observables are extracted by summing all the events within $p_p < 200$ MeV/c, the estimates that are reported are average values over this range of target-nucleon momentum and are in general biased estimates of the observables for scattering off the free nucleon. The bias depends on kinematics and on the observable.

We have tried to quantify this bias by performing a linear extrapolation to the free-proton point at $p_p = 0$ GeV/c for each observable and each kinematic bin. Since for some observables, the dependence with p_p does not seem to be linear (see C_z and P_y in Fig. 7), we fitted the two values of lowest p_p. Assuming that the value of each observable at $p_p = 0$ GeV/c is the true value for scattering off a free nucleon, we evaluated the difference between the QF estimate (average over p_p) and the extrapolated estimate at $p_p = 0$ GeV/c. The differences vary from 0.5 to 46%. Similar studies performed on helicity asymmetries of two-pion photoproduction off the bound proton, yield a range of bias from 5 to 15%. Our results show that when using QF polarization observables as estimates for the observables for production off the free nucleon, the dependence of the observable on target-nucleon momentum should not be disregarded. Unbiased estimates can be obtained by extrapolation methods to the free-nucleon point, however these need to be further studied with simulated data.

4 Summary

Here we report a study of the effect of FSI and target-nucleon momentum on polarization observables for exclusive quasi-free scattering off the bound nucleon. The purpose of the study is to evaluate the extent to which, if at all, such results are unbiased estimates of the observables for photoproduction off the free nucleon. Our work is motivated by the fact that the determination of the excited nucleon spectrum relies not only on data taken with free-proton targets, but also with bound-neutron targets. We determined and studied C_x, C_z, and P_y for the $\gamma(p) \rightarrow K^+\Lambda$ reaction, where the proton is bound in the deuteron. For this process, the available statistics in the E06-103 experiment allows us to extract the evolution of the observables with target-proton momentum for different kinematic bins. We use the momentum evolution to assess the standard analysis method of applying a target-nucleon momentum cut to extract QF observables. Our results suggest that the overall contribution of FSI to the QF event sample is of the level of a few percent. We expect this value to vary with kinematics and to be different for different reactions. While theoretical models can be, and have been, used to correct the unpolarized cross sections for this effect, the determination of any corrections to polarization observables, or their need, is not so clear. Our study shows that the shape of the dependence of the polarization observables on target nucleon momentum is important for the estimate of the observables off the free nucleon and should be taken into account whenever the available statistics allows it. Selecting QF events with small target-nucleon momentum, such as < 200 MeV/c, and disregarding the momentum dependence can yield an estimate that is biased compared to the estimate obtained by extrapolation to the free-nucleon point of 0 MeV/c. More studies using simulated data will allow for a better understanding of this effect.

References

1. B.A. Mecking et al., Nucl. Instrum. Methods A **503**, 513 (2003)
2. P. Nadel-Turonski *et al.*, Jefferson Lab Experiment, Virginia, pp. E06-103 (2006)
3. D.I. Sober et al., Nucl. Instrum. Methods A **440**, 263 (2000)

4. T. Cao, Determination of the Polarization Observables C_x, C_z, and P_y for Final-State Interactions in the Reaction $\gamma d \rightarrow K^+ \Lambda n$, Ph.D. Dissertation, University of South Carolina (2016)
5. M. Lacombe et al., Phys. Rev. C **21**, 861 (1980)
6. E. Wolin, *GSIM User's Guide Version 1.1* (Jefferson Lab, Virginia, 1996)
7. P.T. Mattione et al., Phys. Rev. C **96**, 035204 (2017)